Langmuir

Article

pubs.acs.org/Langmuir

New Approaches for Bottom-Up Assembly of Tobacco Mosaic Virus-Derived Nucleoprotein Tubes on Defined Patterns on Silica- and Polymer-Based Substrates

Carlos Azucena,*[,†,#] Fabian J. Eber,*[,∥,#] Vanessa Trouillet,[‡] Michael Hirtz,[§] Stefan Heissler,[†] Matthias Franzreb,[†] Harald Fuchs,[§,⊥] Christina Wege,[∥] and Hartmut Gliemann[†]

[†]Institute of Functional Interfaces (IFG), [‡]Institute of Applied Materials - Material Process Technology (IAM-WPT), and [§]Institute of Nanotechnology (INT) & Karlsruhe Nano Micro Facility (KNMF), Karlsruhe Institute of Technology, Hermann-von-Helmholtz-Platz 1, 76344 Eggenstein-Leopoldshafen, Germany

[∥]Institute of Biology, University of Stuttgart, Pfaffenwaldring 57, 70550 Stuttgart, Germany

[⊥]Physical Institute & Center for Nanotechnology (CeNTech), Westfälische Wilhelms-Universität, Münster, Germany

Supporting Information

ABSTRACT: The capability of some natural molecular building blocks to self-organize into defined supramolecular architectures is a versatile tool for nanotechnological applications. Their site-selective integration into a technical context, however, still poses a major challenge. RNA-directed self-assembly of tobacco mosaic virus-derived coat protein on immobilized RNA scaffolds presents a possibility to grow nucleoprotein nanotubes in place. Two new methods for their site-selective, bottom-up assembly are introduced. For this purpose, isothiocyanate alkoxysilane was used to activate oxidic surfaces for the covalent immobilization of DNA oligomers, which served as linkers for assembly-directing RNA. Patterned silanization of surfaces was achieved (1) on oxidic surfaces via dip-pen nanolithography and (2) on polymer surfaces (poly(dimethylsiloxane)) via selective oxidization by UV-light irradiation in air. Atomic force microscopy and X-ray photoelectron spectroscopy were used to characterize the surfaces. It is shown for the first time that the combination of the mentioned structuring methods and the isothiocyanate-based chemistry is appropriate (1) for the site-selective immobilization of nucleic acids and, thus, (2) for the formation of viral nanoparticles by bottom-up self-assembly after adding the corresponding coat proteins.

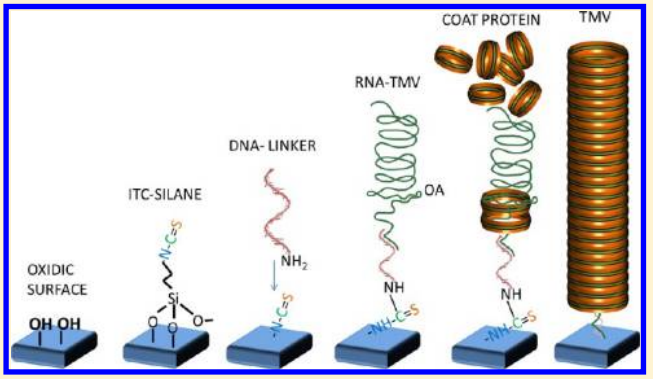

1. INTRODUCTION

The high-throughput preparation of nanosized objects with precisely oriented functional groups in high densities is a large challenge, particularly when the resulting products need to be identical in shape, dimensions, and functionality. Self-assembly is the usual method of nature in creating nanostructured biological devices with high precision. Tobacco mosaic virus (TMV) particles, for example, consist of a well-defined number of coat protein units arranged around a viral RNA in an exactly predetermined geometry. Such directed organization of biological building blocks is one example of how various nanoarchitectures are created in nature with high precision. A scaffold molecule directs the assembly of biopolymers in a well-defined orientation, just driven by the specific interactions between the different components. Coat protein (CP) subunits of TMV arrange precisely on a single viral genomic (scaffolding) RNA to form biological nanotubes both inside plant cells and in vitro.[1−4] An RNA motif located internally but close to the 3′ end in the TMV's genome was shown to present a high affinity toward a preassembled aggregate (disk) made of 34 subunits of the CP of TMV. Different in vitro studies revealed the generally accepted model that at this origin of assembly (OA) site assembly is initiated and then proceeds bidirectionally. For a comprehensive review of this process, see Buttler et al.[5]

The length of the resulting tube-shaped plant virus amounts to 300 nm, which is determined by the length of the underlying RNA (6395 nucleotides).[6] The nucleoprotein nanotube furthermore has an outer diameter of 18 nm and a hollow channel with a diameter of 4 nm. These properties, together with the lack of infectivity for animals and humans and its robustness, offer a high potential for the application of the particles as biotemplates for the production of metallic nanorods[7−9] or virus-based light harvesting systems.[10] Furthermore, the protein coat of the nanotube can be modified by means of genetic engineering and chemical coupling to

Received: July 10, 2012
Revised: August 31, 2012
Published: September 5, 2012

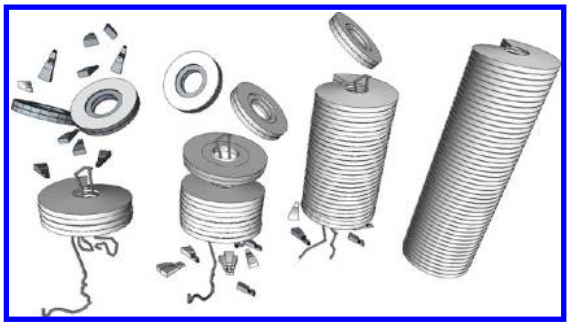

Figure 1. Self-assembly process of TMV as it takes place in a solution containing the RNA template as a scaffold. The virus is formed using the RNA as a guide for preassembled coat protein aggregates.

create structures with different scaffolding characteristics.[11,12] To integrate biological architectures into nano- and microdevices, their deposition is an important construction step. TMV particles can be either randomly attached via the full length of their protein coat[13,14] or fixed via one pole[15−17] to the substrate. Immobilization in a directed way might be useful for the generation of nanocircuits, for example, if the position of the structure can be predetermined. Thus, TMV-derived nanotubes have been deposited site-selectively on DNA arrays[18] and DNA-modified electrodes[19] via the hybridization of a DNA adaptor to a partially exposed stretch of viral RNA. A common characteristic of those strategies is the deposition of previously assembled tubes ("growth in place"). By contrast, in the case of carbon nanotubes, their formation directly at the desired site was shown to bring about superior site-selectivity.[20] Similarly, a recently published versatile spatially selective growth-in-place strategy for TMV-like particles (TLPs) has been realized by a two-step in situ assembly of nucleoprotein nanotubes on DNA arrays.[21] Artificially produced RNA containing the OAs was immobilized on DNA-modified substrates via enzymatic ligation before the surface-associated self-assembly of nucleoprotein nanotubes was induced. In this proof-of-principle experiment, it was shown for the first time that an immobilization of the viral RNA before the viral assembly can be carried out on structured substrates and that the assembly of the CP subunits around the RNA is possible afterward. The structuring technique used was polymer blend lithography[22] combined with an aldehyde-based coupling strategy; however, the created patterns were arbitrarily ordered and the surface density of assembled TLPs was relatively low (quantification).[21]

To create dense arrays of TMV-like particles in defined patches with high reproducibility, we therefore describe new routes for their site-selective bottom-up assembly.

The novel aspects are (1) the application of isothiocyanate (ITC)-based chemistry to immobilize the viral RNA, which allows the preparation of a high surface density of self-assembled TLPs, (2) the combination of ITC chemistry with UV lithography and dip-pen nanolithography (DPN),[23] which allows exact control of the shape and size of the assembly nucleation sites on the substrates, (3) the transfer of ITC-based chemistry to PDMS, which is a polymeric standard material of microfluidic devices for applications in the fields of lab-on-a-chip technology, and (4) the use of DNA/RNA hybridization for the immobilization of assembly-directing RNA to DNA on modified substrates. For surface characterization, X-ray photoelectron spectroscopy (XPS) and atomic force microscopy (AFM) were performed.

2. MATERIALS AND METHODS

2.1. Sample Preparation. Aminopropyltrimethoxysilane (96%) was purchased from ABCR (Germany) and used without any further purification. Synthesis-quality methanol (dry) and toluene (dry) were purchased from VWR, Germany.

Silicon wafers ((100) orientation, polished, diameter 100 ± 5 mm, dotted with borum, specific resistivity 8−12 Ω/cm, thickness 525 ± 20 μm, purchased from Silchem Handelsgesellschaft GmbH, Germany) were cut into 1 × 1 cm^2 pieces, cleaned in a solution of deionized water (Milli-Q, 18.2 MΩ cm, Millipore GmbH, Germany), NH_3, and H_2O_2 (both from Merck, Germany) in a volume ratio of 5:1:1 for 30 min at 70 °C, and then rinsed with Milli-Q water. Afterward, they were subjected to a second acid cleaning with piranha solution prepared in a volume ratio 5:1:1 $H_2O/H_2O_2/H_2SO_4$ (Sigma-Aldrich, Germany) at 70 °C for 30 min. After the cleaning, they were again rinsed with Milli-Q water and left inside the container under water to avoid any contact with air. These wafers were used as substrates for all following experiments. The silanization of the silicon wafers was carried out according to the method of Zeira et al.[24] Silicon wafers previously cleaned and stored in water were silanized using a volume fraction of 3% 3-isothiocyanate-propyl-trimethoxysilane (ITCPTMS) solution in dried methanol. Either commercially available ITCPTES from ABCR or in-house-synthesized ITCPTMS (according to Kaluza[25]) was used indistinctively. The latter was prepared on the basis of the experimental methods of Kaluza and, more recently, Hodgkins,[26,27] who showed that carbethoxydithiocarbamates, which are intermediates in the process of converting an amino group to isothiocyanate, are decomposed into isothiocyanates readily at room temperature by aqueous alkali or by triethylamine in chloroform solution.[26,27] The conversion of a 3-aminopropyl trimethoxy silane into a 3-isothiocyanate-propyl-trimethoxysilane (ITCPTMS) following the Kaluza reaction was performed.

Silanization was carried out by dipping the sample into the ITCPTMS solution for 15 min. Subsequent washing with pure methanol for 2 min was followed by an 8 h cure at 40 °C. Both steps were supported by ultrasonification in order to avoid any physisorption effects of the silane on the surface. This procedure was repeated three times.[24] For functionalization of the DPN-substrates and PDMS substrates, commercially synthesized 3-isothiocyanate propyl triethoxy silane (from ABCR, Germany) was used.

Poly(dimethylsiloxane) (PDMS, Sylgard 184 elastomer from Suter-Kunststoffe AG, Switzerland)-based patterned substrates were prepared according to the following procedure: a drop consisting of PDMS and a cross-linker, prepared in a volume ratio of 10:1, was placed onto a previously cleaned silicon wafer. The sample was hardened over a curing time of 2 h at 70 °C and was used afterward to carry out oxidative patterning by UV irradiation. Patterning was achieved by placing transmission electron microscope (TEM) grids (nickel grids with 400 square mesh and copper grids with 200 square mesh from Plano, Germany) on top of the PDMS substrates and placing them in a UV/ozone chamber (ProCleaner from Bioforce, USA) for 10 h in air. Afterward, the substrates were immediately silanized by dipping them in a solution with a volume fraction of 3% 3-isothiocyanate-propyl-triethoxysilane in dried methanol for 2 h. By this treatment, site-selective silanization of the oxidized areas of the PDMS sample was achieved.

DPN with ITCPTES was performed on glass square coverslips (18 × 18 mm^2, VWR, Germany) that were cleaned by serial ultrasonication in chloroform, isopropanol, and Milli-Q water for 10 min each. After that, the coverslips were blow-dried with nitrogen and DPN was performed using a NLP 2000 (NanoInk Inc., USA). One-dimensional cantilever arrays (F-Type, NanoInk Inc., USA) with 26 cantilevers in a pitch of 35 μm were dipped into pure ITCPTMS, and the excess was blown away with a nitrogen gun. Patterns of 5 dots × 5 dots separated by 5 μm were written with a dwell time of 0.5 s and at a controlled relative humidity of 30 ± 1% rH at a temperature of 25.0 ± 0.5 °C. After silanization, the silicon wafers, the patterned glass slips, and the structured PDMS samples were ready for biofunctionalization.

dx.doi.org/10.1021/la302774h | *Langmuir* 2012, 28, 14867−14877

2.2. DNA Linker Immobilization on ITC-Functionalized Wafers. Generally, from this step on, Milli-Q water that had been treated with dimethyldicarbonate (DMDC, Merck, Germany)[28] was used for the preparation of aqueous solutions. A single-stranded DNA oligomer (ssDNA, purchased from Metabion, Germany, nucleotide sequence ″5′-T_{15}-GCACCACGTGTGATTACGGACACAATCCG-3″) with 5′-terminal amino modification (5′ C6 aminolink) was covalently bound to the isothiocyanate-functionalized areas of the wafers and the PDMS. The linker DNA oligomers were diluted in 1 M Tris-HCl buffer at pH 7.0, 1% *N*,*N*-diisopropylethylamine (DIPEA)[29] to a concentration of 10 pmol/μL. Two microliters of this spotting solution was applied to the functionalized surfaces. After incubation in a humid chamber for 16 h, the surfaces were washed and blocked as reported.[29] Briefly, immobilization was followed by immersion in DMDC-treated Milli-Q water two times for 2 and 5 min in methanol under gentle agitation. Subsequently, the specimens were dried under a stream of nitrogen, and residual isothiocyanate functionalities were blocked by treating them with a solution of 50 mM 6-amino-1-hexanol in DMF containing 150 mM DIPEA for 2 h. After the final washing steps in DMF (2 min), in acetone (2 min), and in DMDC-treated Milli-Q water (two times for 5 min), the specimens were dried under a stream of nitrogen.

2.3. Hybridization of Assembly-Directing RNA and Surface-Associated Assembly of TMV CP. All aqueous buffers were filtered sterile through a 0.2 μm membrane immediately before use. RNA was transcribed in vitro with a MEGAscript Kit (Ambion, Austin, TX) following the manufacturer's protocol. As a template, a shortened derivative of plasmid p843pe35TMVr.1′[12] was created by enzymatic restriction hydrolysis. The formation of an additional SnaBI restriction site, which resulted from mutation T3391C in one of the clones, was used to create a deletion by enzymatic restriction hydrolysis with *Sna*BI (New England Biolabs (NEB), USA) and religation (T4 DNA ligase, NEB). The resulting plasmid p843peTMVΔ9353-3391 was used as a template for transcription after linearization with *Bsi*WI (NEB). This resulted in a 2884-nts-long RNA molecule containing the OAs of TMV and a 3′ end sequence complementary to the linker DNA oligomer. For hybridization to the surface-bound DNA oligomers, a solution of 50 ng/μL RNA final concentration (fc) was first partially denatured in 3× saline-sodium citrate (3xSSC) buffer[30] at 65 °C for 5 min. After the addition of murine RNase inhibitor (NEB) to 1 U/μL fc, 20 μL of this hybridization solution was applied per cm^2 surface area and covered with a baked glass coverslip. Hybridization was performed for about 20 h at 37 °C in a humid chamber. After three washing steps in 2× SSC containing a mass fraction of 0.2% of SDS, 2× SSC, and 0.2× SSC each for 10 min, the RNA-equipped substrates were equilibrated in 75 mM sodium−potassium phosphate (SPP) buffer. TMV CP was prepared from virus particles[2,31] isolated from infected plants[32] and incubated for at least 48 h in 75 mM SPP buffer at pH 7.2 and room temperature at a concentration of 10 mg/mL. To induce assembly, 40 μL of 1.3 mg/mL TMV CP in 75 mM SPP buffer at pH 7.2 was applied to a coverslip per cm^2 of RNA-equipped surfaces. The wafer was placed upside down on a drop of TMV CP solution on a glass coverslip and incubated in a humid chamber for about 20 h. After assembly, the surfaces were washed twice for 3 min in a solution containing a mass fraction of 0.1% SDS and rinsed again twice for 10 min in water before they were dried under a stream of nitrogen and analyzed by AFM.

2.4. Control Experiments. For all experiments, a 2.0 μL drop of the DNA-linker solution was added to the center of the wafer and incubated for 18 h in a humid chamber to avoid any drying effects. After the incubation period, the sample was first washed according to the procedure explained above. Then the RNA was hybridized. Finally, the sample was washed again and a solution containing the CP was applied. Therefore, two different areas can be distinguished: (i) the area that was wetted by the DNA-containing drop and (ii) the area around the DNA-containing drop, which underwent every procedure except DNA addition.

2.5. Sample Characterization. Images were obtained using an Asylum Research atomic force microscope, MFP-3D BIO. The AFM was operated at 25 °C in an isolated chamber in intermittent contact mode. Three types of AFM cantilevers from Ultrasharp MikroMasch were used: an NSC-35 (resonance frequency 315 kHz, spring constant 14 N/m), an NSC-36 (resonance frequency 105 kHz, spring constant 0.95 N/m), and an NSC-18 (resonance frequency 75 kHz, spring constant 3.5 N/m).

X-ray photoelectron spectroscopy (XPS) measurements were performed using a K-Alpha XPS spectrometer (ThermoFisher Scientific, East Grinstead, U.K.). Data acquisition and processing using the Thermo Avantage software are described elsewhere.[33] All thin films were analyzed using a microfocused, monochromated Al K_α X-ray source (400 μm spot size). The kinetic energy of the electrons was measured with a 180° hemispherical energy analyzer operated in the constant analyzer energy mode (CAE) at a 50 eV pass energy for elemental spectra. The K-Alpha charge compensation system was employed during analysis using electrons of 8 eV energy and low-energy argon ions to prevent any localized charge buildup. The spectra were fitted with one or more Voigt profiles (BE uncertainty ± 0.2 eV), and Scofield sensitivity factors were applied for quantification.[34] All spectra were referenced to the C 1s peak of hydrocarbon at a 285.0 eV binding energy controlled by means of the well-known photoelectron peaks of metallic Cu, Ag, and Au.

Fourier-transform infrared spectroscopy (FT-IR) was also performed on some samples to determine if the silane was properly synthesized and compared with isothiocyanate groups in other IR spectra. A Vertex 80 FT-IR spectrometer (Bruker Optik, Ettlingen, Germany) was used with an Hg−Cd−Te narrow-band detector and liquid nitrogen cooling.

3. RESULTS AND DISCUSSION

In the first step, the hydroxyl-terminated silica surface was functionalized with 3-isothiocyanate-propyl-trimethoxysilane

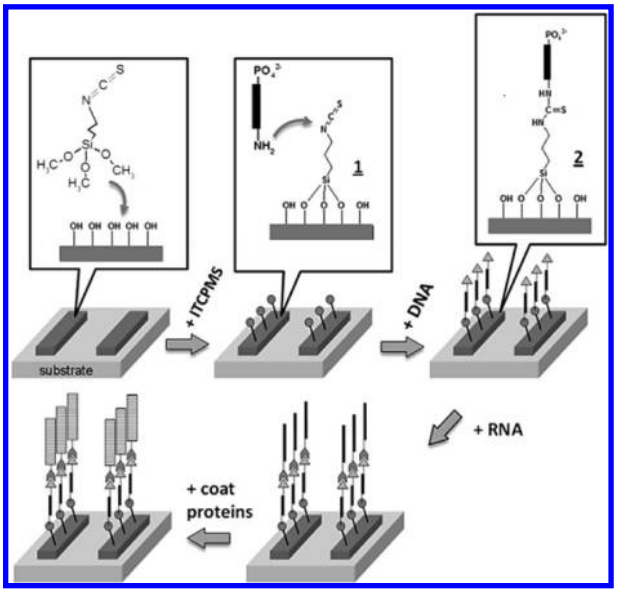

Figure 2. Scheme of the site-selective bottom-up assembly of TMV-like nanoparticles on oxide substrates. After ITC-silane was coupled to the OH-terminated surface patterns, an amino-terminated DNA was coupled, forming a thiourea bond. A complementary-ending RNA strand was immobilized via hybridization, and finally the coat proteins were added for TLP assembly.

(ITCPTMS). Isothiocyanate compounds form stable thiourea bonds with amines. This reaction is almost entirely selective for primary amino groups from lysine side chains and N-terminal α-amines in proteins.[35,36] In the second step, amino-terminated single-stranded DNA oligomers were immobilized covalently to the isothiocyanate groups of the substrate by the formation of

dx.doi.org/10.1021/la302774h | *Langmuir* 2012, 28, 14867−14877

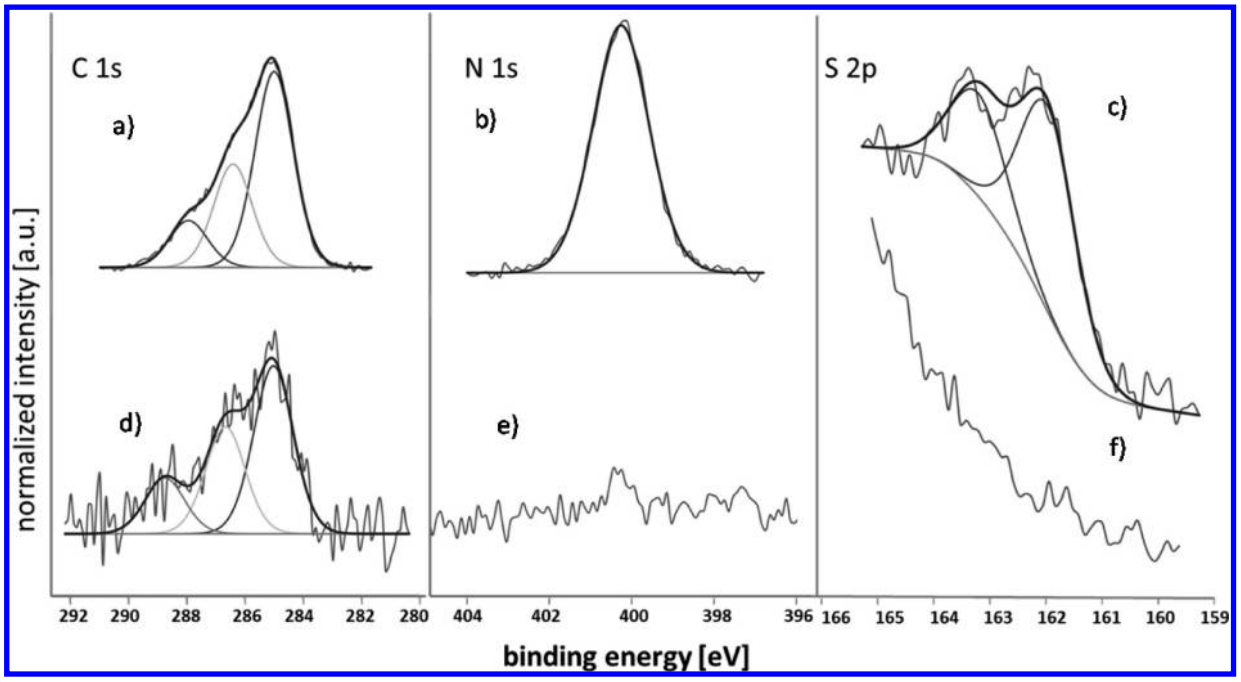

Figure 3. XPS spectra of a silica wafer showing C 1s, N 1s, and S 2p (a–c) after and (d–f) before silanization with ITC silane.

thiourea bonds. After the viral RNA molecules had been hybridized to the DNA anchors, the coat protein was added to form TMV-like particles by self-assembly. Figure 2 schematically shows the process of the (site-selective) bottom-up growth of TMV-like particles used for this work. Because the whole process is based on the functionalization of the supporting substrates with ITC-silane, XPS on silicon wafers and on the oxidized PDMS substrates was used to prove the successful coupling of ITC-silane to the oxide surfaces.

3.1. Nonstructured Silicon Wafers for TLP Assembly. To prove the successful coupling of the ITC silane to the nonstructured silicon substrate, XPS investigations were carried out to compare the C 1s, N 1s, and S 2p signals after (Figure 3a–c) and before (Figure 3d–f) silanization. A pronounced increase in signal intensity for all three atoms is observed after silanization. The C 1s spectrum shows three components: one at 285.0 eV that is assigned to C–C and C–H bonds, one at 286.5 eV that corresponds to –C–N bonds,[37] and one at 288.6 eV that is attributed to O=C–O bonds. After the silanization, the intensity of the nitrogen signal at 400.4 eV increases significantly and can be correlated to –N=C=S bonds.[37] The S 2p doublet with S $2p_{3/2}$ at 162.1 eV can be attributed to the ITC group.

Figure 4a shows the AFM topography image of the structures formed after ITC functionalization of the silicon substrate, coupling of the DNA linker, RNA hybridization, and addition of a coat protein. Bottom-up assembly of the viruslike tubes, shown as elevated, elongated nanoparticles on the silicon wafer substrates, was successful (Figure 4a). A high density of rod-shaped nanostructures was formed in a reproducible way. The optimized preparation method was thus suitable for further investigations.

The length distribution of the TMV-like particles is shown in Figure 4b. The average length was 85 nm with a standard deviation of ±30 nm. Upon AFM investigation, the TMV-like particles consistently had the same height of 12 nm, which is not in agreement with the theoretical diameter of 18 nm. This can be explained (1) by the flattening of the particles after drying when the protein coat comes into contact with the surface and, to a minor extent, (2) by a deformation of the particle due to the vertical force that is applied to the particles by the AFM tip during measurement. For statistical evaluation, only those TLPs with a height profile of approximately 12 nm were taken into account. The predicted maximal length of 135 nm, as determined from the length of the RNA used in this investigation, was rarely achieved. Approximately 40 % of the evaluated TLPs had lengths of between 70 and 90 nm, 20% had lengths of between 100 and 120 nm, and 12% had lengths of between 130 and 150 nm. Very few were found to be longer than 160 nm (3%) (Figure 4b). The discrepancy between the expected and the observed particle lengths may be explained by an interaction between the nascent particles and the substrate or by blocked, nonaccessible sites along the RNA.[21] The particles with lengths of between 40 and 60 nm can be considered to be incompletely assembled.

To prove that the bottom-up assembly of the nucleoprotein rods on the substrate was due to neither unspecific adsorbed DNA linkers nor RNA scaffolds, respectively, nor due to the adsorption of TMV-like particles potentially preassembled in solution, a set of control experiments were carried out. As described in the Materials and Methods section (control experiments), in all experiments a drop of the DNA-linker solution was added to the center of the wafer and processed later. As a consequence, generally two different areas could be distinguished: (i) the area wetted by the DNA-containing drop (corresponding to Figure 4a) and (ii) the area around it, which followed every step except the DNA addition. On areas lacking the DNA layer, no TMV-like particles could be recognized on the substrate (Figure 4c). In a further control experiment, the step of RNA coupling via hybridization was skipped during sample preparation, whereas the samples were otherwise treated with both the DNA and CP solutions as above. The AFM topography image of Figure 4d represents the corresponding sample surface: no TMV-like rods were found, which proves that without RNA the self-assembly process of TMV CP did not occur. Furthermore, viruslike particles grown

dx.doi.org/10.1021/la302774h | *Langmuir* 2012, 28, 14867–14877

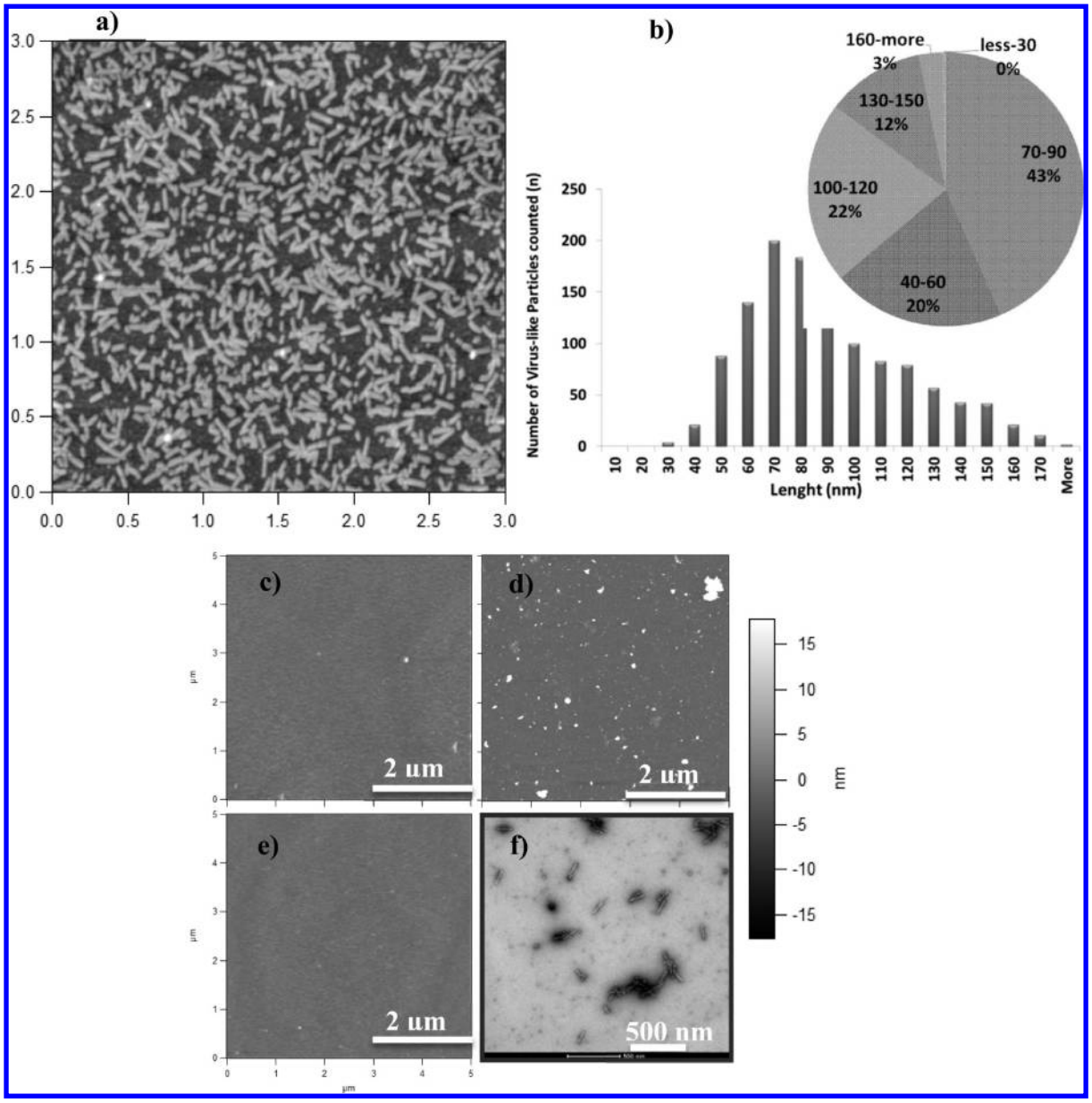

Figure 4. Self-assembly of TMV-like nanorod structures on ITC-terminated silicon substrates. Representative AFM topography images (brightness scale is the same for all the images) of a substrate (a, b) coated with self-assembled TMV-like particles after all preparation steps, (c) which was prepared by skipping the treatment with DNA, (d) after adding DNA and CP but avoiding RNA treatment, and (e) after a solution of preassembled particles was dropped and dried. (f) TEM image of the preassembled TMV-like particles. (b) Statistical analysis of the particle length based on part a.

in solution were incubated with as-prepared surfaces. The protein coat of these preassembled particles did not interact with the functionalized surface. As a result, no TMV-like particles were detected (Figure 4e), although a TEM investigation of the solution that contained the preassembled viral nanorods prove their successful assembly (Figure 4f). Thus, several conclusions can be drawn: (i) no unspecific physisorption of assembly-directing RNA takes place on accordingly prepared surfaces, (ii) no unspecific induction of assembly triggered by the interaction of TMV CP with the surface occurs, and (iii) assembly takes place in a surface-associated fashion and not in solution, followed by the physisorption of newly formed particles.

3.2. Site-Selective Assembly of TMV CP on Silicon Wafers Structured by Dip-Pen Nanolithography. The chemical one-step coupling of ITC-silane to the oxide surface of the substrate offers the opportunity to apply DPN to create arrays of ITC-terminated spots on glass coverslips. With this method, not only can the size and the distance between the functionalized spots be reduced to submicrometer dimensions but also the density and the shape of the structures can be varied arbitrarily. (For further reading, see refs 23 and 38−40.) The pattern created by DPN makes it easy to re-find exactly the same spots after each preparation step. Figure 5 shows AFM topography images of a 5 spot × 5 spot array after the deposition of ITCPTMS droplets by DPN (Figure 5a), after the coupling of the DNA linkers to the silanized areas (Figure 5c) and after the self-assembling process of the TMV-like particles (Figure 5e). A preliminary assessment of the substrates was performed by optical inspection using amino fluorescein coupling to verify the distribution, order, and reactivity of silane toward amino groups (not shown). The experiment indeed

dx.doi.org/10.1021/la302774h | *Langmuir* 2012, 28, 14867−14877

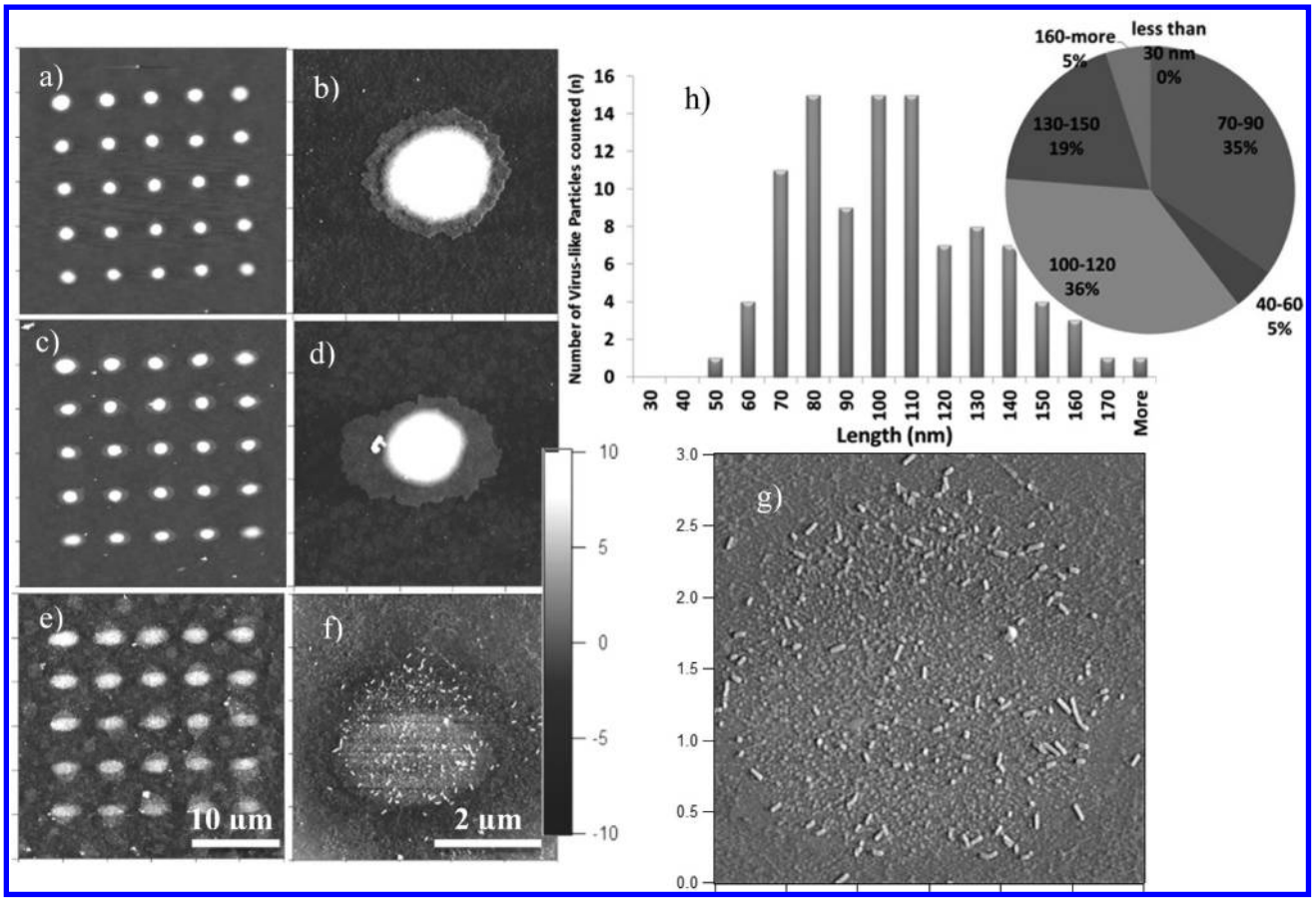

Figure 5. AFM topography images of (a) a 5 × 5 array of ITC-terminated spots after the deposition of ITCPTES by DPN on a glass slide, (c) after coupling with linker DNA, and (e) after TLP self-assembly. (b, d, f) Magnification of individual spots in parts a, c, and e, respectively. A higher magnification of image f and a statistical evaluation of the length distribution of TMV-like particles are shown in parts g and h.

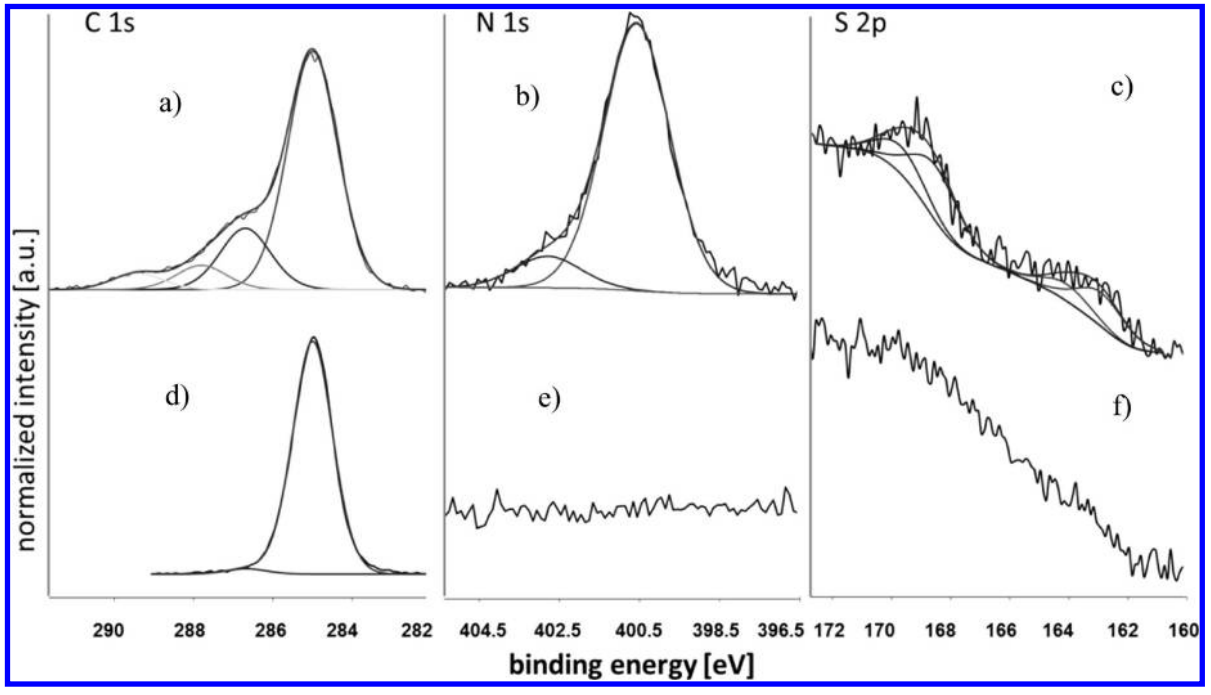

Figure 6. XPS spectra of (a–c) ITC-functionalized PDMS substrates and (d–f) nontreated PDMS.

showed specificity with a clear preference for the silanized areas. The spots shown in Figure 5a,b have an average height of 25 nm. This is significantly higher than would be expected for a monolayer of ITC-silane on the surface. However, in contrast to the preparation of the ITC-terminated Si wafers as described before, the deposition of small ITC-silane droplets on the glass

dx.doi.org/10.1021/la302774h | *Langmuir* 2012, 28, 14867–14877

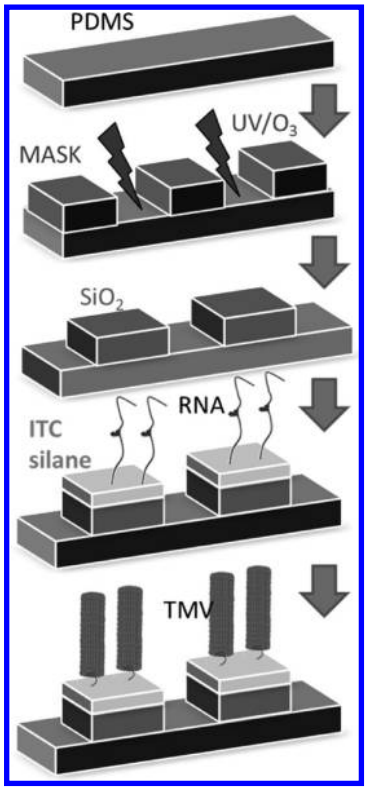

Figure 7. Schematic process of the site-selective bottom-up assembly of TMV-like nanotube particles on oxidized PDMS patterns, which were prepared by UV-light irradiation of the polymer surface through a mask. After irradiation, the ITC-silane is attached to the OH-terminated surface patterns and an amino-terminated DNA is coupled, forming a thiourea bond. A complementary-ending RNA strand is immobilized, and finally the coat proteins are added for TLP assembly.

by the DPN method occurred in air with a relative humidity of 30%. Under these conditions and without any washing or rinsing step, all deposited molecules can polymerize and thus form an ITC-silane multilayer, which explains the observed height. The polymerization of silanes under high humidity is well-known in the literature.[41]

After the coupling of the DNA linker (Figure 5c,d), the hybridization of RNA strands and the induction of assembly by the addition of TMV CP were performed, and a significant decrease in the height of the spotted areas from 25- to 10-nm-high plateaus could be observed. This is probably due to the removal of parts of the polymerized noncovalently bound material by several washing steps during RNA immobilization and the assembly of the nucleoprotein tubes. TMV-like particles were formed specifically on the areas of the plateaus (Figure 5f). As there was no unspecific adsorption of the assembly-directing RNA to the silanized surface without DNA detected (Figure 4c), the appearance of TMV-like particles, which have the same dimensions as the particles obtained from the other experiments, on the spotted areas proves that a site-selective permanent immobilization of DNA oligomers took place on the silanized spots. The surface density of particles decreased from the rim of the spot to its center, which can be seen in the close-up image in Figure 5g. This density gradient of the particles can be explained by the diffusion of the DNA-containing solution underneath the polymerized silane, which was just loosely bound to the substrate and was washed away during the subsequent preparation steps. The DNA thus was immobilized by those ITC-terminated silane molecules that were covalently bound to the glass substrate and were not removed during the washing procedures. In Figure 5h, the statistical analysis of the length distribution of the TMV-like particles is shown. Approximately 35% of the evaluated particles had lengths of between 70 and 90 nm, 36% had lengths of between 100 and 120 nm, and 19% had lengths of between 130 and 150 nm. Very few were found to be longer than 160 nm (5%).

3.3. Site-Selective Assembly on PDMS Structured by UV-Light Lithography. Motivated by the functionalization of silica surfaces with isothiocyanate-terminated silanes as base substrate for the bottom-up assembly of TMV-like particles, we transferred this chemistry to polymeric substrates based on poly(dimethylsiloxane) (PDMS), a polymer that is often used as a material for microfluidic or lab-on-a-chip devices. In the following text, the coupling of the ITCPTES and the bottom-up assembly of TMV-like particles to oxidized PDMS is introduced.

The irradiation of PDMS with UV light in an oxygen-containing atmosphere allows the oxidation of the $-CH_3$ groups in the upper layers of the polymeric bulk. UV light with a maximum emission at 254 nm can be used to cleave the bonds of organic molecules on surfaces.[42−44] Strong emission at 185 nm converts atmospheric oxygen into reactive ozone, which in turn attacks the methyl groups and creates volatile organics. In this case, the $-CH_3$ group of the silicon polymer is oxidized to −COOH, −COH, or −OH, resulting in a chemically modified, hydrophilic, silicalike layer on the top of the polymer substrate.[45−48] This fact has already been studied by Genzer,[49] Chaudhury,[50,51] Ferguson,[52] and others,[53] and they already used silanes for coupling to polymeric substrates, whereupon the hydroxyl groups are used for the coupling to the ITC-terminated silane.

It is known that hydrophobicity recovery can be observed for PDMS substrates that have been modified under irradiation with UV/O_3 in a time interval of 2 h. The recovery was explained as being due to the diffusion of nonoxidized low-molar-mass PDMS through cracks in the silica-like surface layer.[53−56] Toth et al.[57] studied silicone rubber surfaces exposed to radio-frequency (rf) plasma or corona discharges in air. They found that silica-like layers formed on the surface, with a thickness of less than 3 nm, using angle-resolved XPS. They concluded that the diffusion of low-molar-mass PDMS played a more important role in the hydrophobicity recovery than the reorientation of polar groups in the bulk of the rubber. The importance of these phenomena lies in the stability of the brittle layer of silica on top. Therefore, for the experiments described here an irradiation time of 10 h was chosen to make sure (i) that SiO_2 is formed on top of the PDMS (Waddell et al.)[42,43,58−62] and (ii) that the formed SiO_2 layer is thick enough to avoid the recovery of the inorganic material. To prove that the SiO_2 established on top of the PDMS behaves in a chemically identical manner to the SiO_2 wafer,[48,63,64] XPS experiments were carried out before and after the treatment of irradiated PDMS with ITCPTES. In Figure 6, the C 1s, N 1s, and S 2p signals before (Figure 6d−f) and after silanization (Figure 6a−c) are shown. The presence of nitrogen and sulfur in the spectra of the silanized PDMS (Figure 6b,c) relative to the nontreated PDMS (Figure 6e,f), respectively, confirms the functionalization of the surface with the isothiocyanate group. Also, the C 1s peak (Figure 6a) can be deconvoluted into several components {285.0 eV (C−C, C−H), 286.7 eV (C−O,

dx.doi.org/10.1021/la302774h | *Langmuir* 2012, 28, 14867−14877

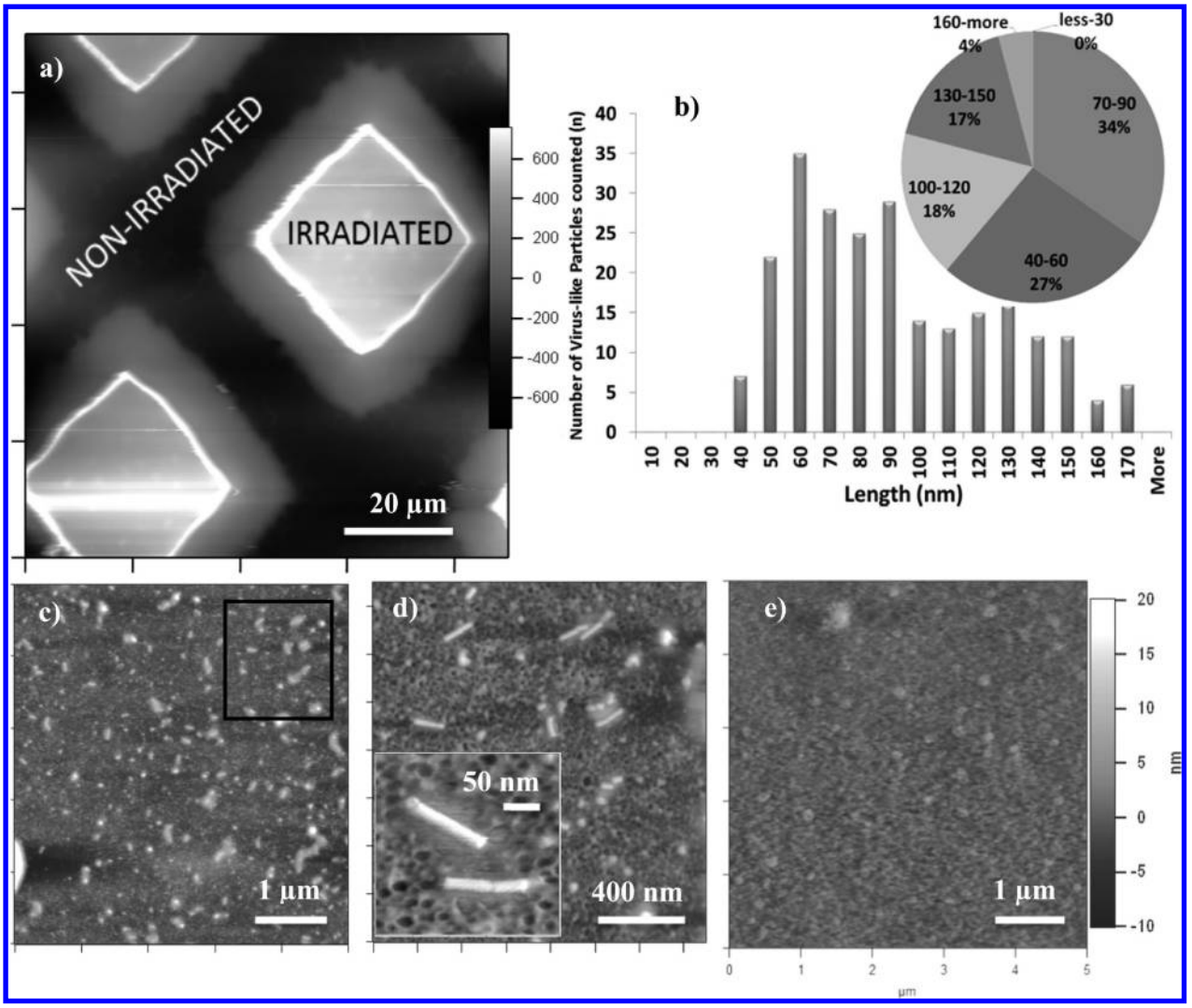

Figure 8. (a) AFM topography images of a PDMS substrate after irradiation through a mask and the complete process of TLP assembly. The AFM topography images (c and d) show details of the irradiated areas at different magnifications after TLP growth. The inset in part d shows a magnification of single TLPs from another area of the same sample. (e) No TLPs can be detected in the non-irradiated area. (b) Statistical analysis of TLP lengths.

C−N), 287.8 eV (N═C═S), and 289.4 eV (O−C═O)} that are in agreement with the experiments of Graf.[37] These components indicate the presence of ITCPTES but also show the oxidation of the molecule. The S 2p doublet at 163.2 eV shows the presence of isothiocyanate whereas the doublet at 169.0 eV (Figure 6c) also hints at oxidation.[65] In our case, the N 1s peak (Figure 6b) can be deconvoluted into two components: one near 402.8 eV that is characteristic of protonated[66] primary amino groups and another at 400.6 eV that can be attributed to the −N═C═S bond.[37,67]

The XPS results prove that the oxide layer, prepared by the irradiation of PDMS with UV light, shows the same chemical behavior as the SiO_2 wafer and in both cases the ITC-terminated silane can be covalently coupled. To achieve site-selective TLP assembly on a polymeric substrate, a PDMS substrate was irradiated with UV light through a mask to produce a selectively oxidized polymer substrate. An irradiation time of 10 h was chosen to avoid the recovery of the formed SiO_2 with low-molar-mass PDMS, which might influence the TLP assembly. The irradiated polymer substrate was subsequently silanized and used for the bottom-up growth of the TMV-like particles. The whole preparation process is described in the scheme in Figure 7.

The procedure of TLP bottom-up assembly (silanization, DNA coupling, RNA coupling, and assembly of coat proteins) was carried out on the selectively oxidized substrates. Two regions were visible in the AFM topography image shown in Figure 8a: (1) squares in which the conversion from PDMS to the silica-like surface took place and (2) the bars between the squares where the mask hindered the process of oxidation, leaving the polymer unchanged. Several rods were found in the square parts of the irradiated and chemically modified PDMS patterns (Figure 8c,d) whereas on the nonirradiated areas no particles could be detected (Figure 8e). The average lengths of the rods are in agreement with those that were assembled on pure silica wafers. The histogram in Figure 8b shows the results of the particle lengths determined over the 25 μm^2 area of Figure 8c. The average length was around 87 nm with a standard deviation of 34 nm. Although the mean and standard deviation are in agreement with the results from the silica wafer experiments (Figure 4b), a distribution with a more pronounced skewedness toward longer particles was found.

dx.doi.org/10.1021/la302774h | *Langmuir* 2012, 28, 14867−14877

We found that the TMV-like particles self-assembled exclusively on those surface areas that were irradiated and silanized. This indicates a highly selective coupling of the virus RNA on the respective areas. The increased roughness (rms = 1.5 nm) of these PDMS areas as shown in Figure 8c–e compared to those of the silanized Si wafers depicted in Figure 4c (rms = 0.75 nm) might be due to the described hydrophobicity recovery of the polymer during the initial time period of the irradiation process. In Figure 8b, the statistical analysis of the length distribution of the TMV-like particles is shown. About 27% of the evaluated particles had lengths of between 40 and 60 nm, 34% has length of between 70 and 90 nm, 18% has length of between 100 and 120 nm, and 17% has length of between 130 and 150 nm. Very few were found to be longer than 160 nm (4%). It can be concluded that only in the case of the nonstructured Si wafer (Figure 4) can a pronounced maximum in the length distribution of the TMV-like particles of between 70 and 80 nm be detected. In all cases, the determined average lengths of the TMV-like particles are smaller than 135 nm, which would be the expected length of a completely assembled virus particle with a 2884-nts-long RNA molecule, which was used for the investigations. This discrepancy can be due to different reasons, such as the unspecific interaction between "blank" parts of the RNA strand with the surface or steric hindrance during the formation of the protein coat.

The high density of TMV-like particles obtained with silicon surfaces could not be reproduced on PDMS.

4. CONCLUSIONS

From the experiments it can be concluded that (1) the new approach to realizing the bottom-up self-assembly of TMV-like particles on oxide interfaces based on the formation of a thiourea bond between an ITC-terminated substrate and an amino-functionalized linker DNA is successful and (2) bottom-up assembly can be carried out site-selectively on both Si wafers with a native oxide layer and on UV-irradiated PDMS. In addition, we could show that the combination of the ITC-based chemistry with two different structuring techniques—the dip-pen nanolithography and the photo-oxidation of PDMS—results in the site-selective growth of TMV-like particles. Compared to the method described in Müller et al.,[21] the coupling of the aminated DNA linker via the ITC-terminated silanes resulted in a reproducibly high density of the grown TMV-like particles whereas the geometry of the coupling sites could be varied in size and shape in a well-defined manner in the case of dip-pen nanolithography (DPN) and UV lithography of the PDMS material. Because one of the main intentions of this work was to prove that the site-selective growth of TMV-like particles can be realized by combining the bottom-up self-assembly of the TLP with top-down structuring methods, more experiments will be necessary to determine why the different substrate materials and structuring techniques result in different particle densities and/or length distributions. The approach of transferring the ITC-based chemistry for TLP growth to the PDMS material that is used in the preparation of microfluidic devices provides access to many applications in the field of lab-on-a-chip techniques, where TMV-like particles might serve as useful carrier templates of peptides or enzymes for analytical purposes.

■ ASSOCIATED CONTENT

Ⓢ Supporting Information

FTIR spectra from 3-aminopropyltrimethoxysilane and the final product 3-isothiocyanatepropyltrimethoxysilane after Kaluza and Hodgkings reaction. FTIR assignments for the fundamental modes of 3-aminopropyltrimethoxysilane and 3-isothiocyanate-propyltrimethoxysilane. This material is available free of charge via the Internet at http://pubs.acs.org.

■ AUTHOR INFORMATION

Corresponding Author

*Tel: +4972160826435.

Author Contributions

#These authors contributed equally to this work.

Notes

The authors declare no competing financial interest.

■ ACKNOWLEDGMENTS

We thank the Baden-Württemberg Stiftung for funding this research as well as Andre Petershans, Anna Müller, Alexander Bittner, Thomas Schimmel, Stefan Walheim and especially Holger Jeske for their support and valuable discussions. This work was partially carried out with the support of the Karlsruhe Nano Micro Facility (KNMF, www.kmf.kit.edu), a Helmholtz Research Infrastructure at Karlsruhe Institute of Technology (KIT, www.kit.edu).

■ REFERENCES

(1) Klug, A. The tobacco mosaic virus particle: structure and assembly. *Philos. Trans. R. Soc., B* **1999**, *354*, 531–535.

(2) Fraenkel-Conrat, H.; Williams, R. C. Reconstitution of active tobacco mosaic virus from its inactive protein and nucleic acid components. *Proc. Natl. Acad. Sci.* **1955**, *41*, 690–698.

(3) Namba, K.; Stubbs, G. Structure of tobacco mosaic virus at 3.6 A resolution: implications for assembly. *Science* **1986**, *231*, 1401–1406.

(4) Ge, P.; Zhou, Z. H. Hydrogen-bonding networks and RNA bases revealed by cryo electron microscopy suggest a triggering mechanism for calcium switches. *Proc. Natl. Acad. Sci. U.S.A.* **2011**, *108*, 9637–9642.

(5) Butler, P. J. G. Self-assembly of tobacco mosaic virus: the role of an intermediate aggregate in generating both specificity and speed. *Philos. Trans. R. Soc., B* **1999**, *354*, 537–550.

(6) Goelet, P.; Lomonossoff, G. P.; Butler, P. J. G.; Akam, M. E.; Gait, M. J.; Karn, J. Nucleotide sequence of tobacco mosaic virus RNA. *Proc. Natl. Acad. Sci. U.S.A.* **1982**, *79*, 5818–5822.

(7) Chen, X.; Gerasopoulos, K.; Guo, J.; Brown, A.; Wang, C.; Ghodssi, R.; Culver, J. N. Virus-enabled silicon anode for lithium-ion batteries. *ACS Nano* **2010**, *4*, 5366–5372.

(8) Nam, K. T.; Kim, D.-W.; Yoo, P. J.; Chiang, C.-Y.; Meethong, N.; Hammond, P. T.; Chiang, Y.-M.; Belcher, A. M. Virus-enabled synthesis and assembly of nanowires for lithium ion battery electrodes. *Science* **2006**, *312*, 885–888.

(9) Lee, Y. J.; Yi, H.; Kim, W.-J.; Kang, K.; Yun, D. S.; Strano, M. S.; Ceder, G.; Belcher, A. M. Fabricating genetically engineered high-power lithium-ion batteries using multiple virus genes. *Science* **2009**, *324*, 1051–1055.

(10) Dedeo, M. T.; Duderstadt, K. E.; Berger, J. M.; Francis, M. B. Nanoscale protein assemblies from a circular permutant of the tobacco mosaic virus. *Nano Lett.* **2009**, *10*, 181–186.

(11) Wu, Z.; Mueller, A.; Degenhard, S.; Ruff, S. E.; Geiger, F.; Bittner, A. M.; Wege, C.; Krill, C. E., III. Enhancing the magnetoviscosity of ferrofluids by the addition of biological nanotubes. *ACS Nano* **2010**, *4*, 4531–4538.

(12) Kadri, A.; Maiss, E.; Amsharov, N.; Bittner, A. M.; Balci, S.; Kern, K.; Jeske, H.; Wege, C. Engineered tobacco mosaic virus

mutants with distinct physical characteristics in planta and enhanced metallization properties. *Virus Res.* **2011**, *157*, 35−46.
(13) Gerasopoulos, K.; McCarthy, M.; Banerjee, P.; Fan, X.; Culver, J. N.; Ghodssi, R. Biofabrication methods for the patterned assembly and synthesis of viral nanotemplates. *Nanotechnology* **2010**, *21*, 055304−055311.
(14) Royston, E.; Ghosh, A.; Kofinas, P.; Harris, M. T.; Culver, J. N. Self-assembly of virus-structured high surface area nanomaterials and their application as battery electrodes. *Langmuir* **2008**, *24*, 906−912.
(15) Lin, Y.; Balizan, E.; Lee, L. A.; Niu, Z.; Wang, Q. Self-assembly of rodlike bio-nanoparticles in capillary tubes. *Angew. Chem., Int. Ed.* **2010**, *122*, 880−884.
(16) Lin, Y.; Su, Z.; Xiao, G.; Balizan, E.; Kaur, G.; Niu, Z.; Wang, Q. Self-assembly of virus particles on flat surfaces via controlled evaporation. *Langmuir* **2010**, *27*, 1398−1402.
(17) Wang, S.; Fukuto, M.; Checco, A.; Niu, Z.; Wang, Q.; Yang, L. Role of electrostatic interactions in two-dimensional self-assembly of tobacco mosaic viruses on cationic lipid monolayers. *J. Colloid Interface Sci.* **2011**, *358*, 497−505.
(18) Yi, H.; Rubloff, G. W.; Culver, J. N. TMV microarrays: hybridization-based assembly of DNA-programmed viral nanotemplates. *Langmuir* **2007**, *23*, 2663−2667.
(19) Yi, H. M.; Nisar, S.; Lee, S. Y.; Powers, M. A.; Bentley, W. E.; Payne, G. F.; Ghodssi, R.; Rubloff, G. W.; Harris, M. T.; Culver, J. N. Patterned assembly of genetically modified viral nanotemplates via nucleic acid hybridization. *Nano Lett.* **2005**, *5*, 1931−1936.
(20) Nessim, G. D. Properties, synthesis, and growth mechanisms of carbon nanotubes with special focus on thermal chemical vapor deposition. *Nanoscale* **2010**, *2*, 1306−1323.
(21) Mueller, A.; Eber, F. J.; Azucena, C.; Petershans, A.; Bittner, A. M.; Gliemann, H.; Jeske, H.; Wege, C. Inducible site-selective bottom-up assembly of virus-derived nanotube arrays on RNA-equipped wafers. *ACS Nano* **2011**, *5*, 4512−4520.
(22) Walheim, S.; Böltau, M.; Mlynek, J.; Krausch, G.; Steiner, U. Structure formation via polymer demixing in spin-cast films. *Macromolecules* **1997**, *30*, 4995−5003.
(23) Piner, R. D.; Zhu, J.; Xu, F.; Hong, S.; Mirkin, C. A. "Dip-pen" nanolithography. *Science* **1999**, *283*, 661−663.
(24) Zeira, A.; Chowdhury, D.; Maoz, R.; Sagiv, J. Contact electrochemical replication of hydrophilic−hydrophobic monolayer patterns. *ACS Nano* **2008**, *2*, 2554−2568.
(25) Kaluza, L. Über eine neue Darstellungsmethode von Senfölen. *Monatsh. Chem.* **1912**, *33*, 363−371.
(26) Hodgkins, J. E.; Reeves, W. P. The modified Kaluza synthesis. III. The synthesis of some aromatic isothiocyanates. *J. Org. Chem.* **1964**, *29*, 3098−3099.
(27) Hodgkins, J. E.; Ettlinger, M. G. The synthesis of isothiocyanates from amines. *J. Org. Chem.* **1956**, *21*, 404−405.
(28) Jourlin-Castelli, C. Transcriptome Analysis by Microarrays. In *Prokaryotic Genomics*; Blot, M., Ed.; Birkhäuser Verlag: Basel, 2003; pp 145−156.
(29) Manning, M.; Harvey, S.; Galvin, P.; Redmond, G. A versatile multi-platform biochip surface attachment chemistry. *Mater. Sci. Eng., C* **2003**, *23*, 347−351.
(30) Sambrook, J.; Russell, D. W. *Molecular Cloning: A Laboratory Manual.*, 3rd ed.; Cold Spring Harbor Laboratory Press: Cold Spring Harbor, NY, 2001.
(31) Fraenkel-Conrat, H. Degradation of tobacco mosaic virus with acetic acid. *Virology* **1957**, *4*, 1−4.
(32) Gooding, G. V.; Hebert, T. T. A simple technique for purification of tobacco mosaic virus in large quantities. *Phytopathology* **1967**, *57*, 1285.
(33) Parry, K. L.; Shard, A. G.; Short, R. D.; White, R. G.; Whittle, J. D.; Wright, A. ARXPS characterisation of plasma polymerised surface chemical gradients. *Surf. Interface Anal.* **2006**, *38*, 1497−1504.
(34) Scofield, J. H. Hartree-Slater subshell photoionization cross-sections at 1254 and 1487 eV. *J. Electron Spectrosc. Relat. Phenom.* **1976**, *8*, 129−137.
(35) Jorbágy, A.; Király, K. Chemical characterization of fluorescein isothiocyanate-protein conjugates. *Biochim. Biophys. Acta.* **1966**, *124*, 166−175.
(36) Rana, T. M.; Meares, C. F. N-terminal modification of immunoglobulin polypeptide chains tagged with isothiocyanato chelates. *Bioconjugate Chem.* **1990**, *1*, 357−362.
(37) Graf, N.; Lippitz, A.; Gross, T.; Pippig, F.; Holländer, A.; Unger, W. Determination of accessible amino groups on surfaces by chemical derivatization with 3,5-bis(trifluoromethyl)phenyl isothiocyanate and XPS/NEXAFS analysis. *Anal. Bioanal. Chem.* **2010**, *396*, 725−738.
(38) Ginger, D. S.; Zhang, H.; Mirkin, C. A. The evolution of dip-pen nanolithography. *Angew. Chem., Int. Ed.* **2004**, *43*, 30−45.
(39) Salaita, K.; Wang, Y.; Mirkin, C. A. Applications of dip-pen nanolithography. *Nat Nano* **2007**, *2*, 145−155.
(40) Wu, C.-C.; Reinhoudt, D. N.; Otto, C.; Subramaniam, V.; Velders, A. H. Strategies for patterning biomolecules with dip-pen nanolithography. *Small* **2011**, *7*, 989−1002.
(41) Yang, L.; Feng, J.; Zhang, W.; Qu, J.-e. Film forming kinetics and reaction mechanism of γ-glycidoxypropyltrimethoxysilane on low carbon steel surfaces. *Appl. Surf. Sci.* **2010**, *256*, 6787−6794.
(42) Zimmermann, C. G. On the kinetics of photodegradation in transparent silicones. *J. Appl. Phys.* **2008**, *103*, 083547−083549.
(43) Waddell, E. A.; Shreeves, S.; Carrell, H.; Perry, C.; Reid, B. A.; McKee, J. Surface modification of Sylgard 184 polydimethylsiloxane by 254 nm excimer radiation and characterization by contact angle goniometry, infrared spectroscopy, atomic force and scanning electron microscopy. *Appl. Surf. Sci.* **2008**, *254*, 5314−5318.
(44) Morvan, J.; Camelot, M.; Zecchini, P.; Roques-Carmes, C. Infrared investigation of the role of ozone oxidation in the adhesion of polydimethylsiloxane films. *J. Colloid Interface Sci.* **1984**, *97*, 149−156.
(45) Ouyang, M.; Yuan, C.; Muisener, R. J.; Boulares, A.; Koberstein, J. T. Conversion of some siloxane polymers to silicon oxide by UV/ozone photochemical processes. *Chem. Mater.* **2000**, *12*, 1591−1596.
(46) Matienzo, L.; Egitto, F. Transformation of poly(dimethylsiloxane) into thin surface films of SiO_2 by UV/ozone treatment. Part II: segregation and modification of doped polymer blends. *J. Mater. Sci.* **2006**, *41*, 6374−6384.
(47) Egitto, F.; Matienzo, L. Transformation of poly(dimethylsiloxane) into thin surface films of SiO_2 by UV/ozone treatment. Part I: factors affecting modification. *J. Mater. Sci.* **2006**, *41*, 6362−6373.
(48) Efimenko, K.; Wallace, W. E.; Genzer, J. Surface modification of Sylgard-184 poly(dimethyl siloxane) networks by ultraviolet and ultraviolet/ozone treatment. *J. Colloid Interface Sci.* **2002**, *254*, 306−315.
(49) Genzer, J.; Efimenko, K. Creating long-lived superhydrophobic polymer surfaces through mechanically assembled monolayers. *Science* **2000**, *290*, 2130−2133.
(50) Chaudhury, M. K. Surface free energies of alkylsiloxane monolayers supported on elastomeric polydimethylsiloxanes. *J. Adhes. Sci. Technol.* **1993**, *7*, 669−675.
(51) Manoj K, C. Self-assembled monolayers on polymer surfaces. *Biosens. Bioelectron.* **1995**, *10*, 785−788.
(52) Ferguson, G. S.; Chaudhury, M. K.; Biebuyck, H. A.; Whitesides, G. M. Monolayers on disordered substrates: self-assembly of alkyltrichlorosilanes on surface-modified polyethylene and poly(dimethylsiloxane). *Macromolecules* **1993**, *26*, 5870−5875.
(53) Kim, J.; Chaudhury, M. K.; Owen, M. J. Modeling hydrophobic recovery of electrically discharged polydimethylsiloxane elastomers. *J. Colloid Interface Sci.* **2006**, *293*, 364−375.
(54) Blackmore, P.; Birtwhistle, D. Surface discharges on polymeric insulator shed surfaces. *IEEE Trans. Dielectr. Electr. Insul.* **1997**, *4*, 210−217.
(55) Kim, H.; Urban, M. W. Effect of discharge gases on microwave plasma reactions of imidazole on poly(dimethylsiloxane) surfaces: quantitative ATR FT-IR spectroscopic analysis. *Langmuir* **1999**, *15*, 3499−3505.

(56) Kim, J.; Chaudhury, M. K.; Owen, M. J. Hydrophobicity loss and recovery of silicone HV insulation. *IEEE Trans. Dielectr. Electr. Insul.* **1999**, *6*, 695−702.
(57) Tóth, A.; Bertóti, I.; Blazsó, M.; Bánhegyi, G.; Bognar, A.; Szaplonczay, P. Oxidative damage and recovery of silicone rubber surfaces. I. X-ray photoelectron spectroscopic study. *J. Appl. Polym. Sci.* **1994**, *52*, 1293−1307.
(58) Delman, A. D.; Landy, M.; Simms, B. B. Photodecomposition of polymethylsiloxane. *J. Polym. Sci., Part A-1: Polym. Chem.* **1969**, *7*, 3375−3386.
(59) Balykova, T. N.; Rode, V. V. Progress in the study of the degradation and stabilisation of siloxane polymers. *Russ. Chem. Rev.* **1969**, *38*, 306.
(60) Sadhu, V. B.; Perl, A.; Péter, M.; Rozkiewicz, D. I.; Engbers, G.; Ravoo, B. J.; Reinhoudt, D. N.; Huskens, J. Surface modification of elastomeric stamps for microcontact printing of polar inks. *Langmuir* **2007**, *23*, 6850−6855.
(61) Becker, H.; Gärtner, C. Polymer microfabrication methods for microfluidic analytical applications. *Electrophoresis* **2000**, *21*, 12−26.
(62) Xue, C.-Y.; Chin, S. Y.; Khan, S. A.; Yang, K.-L. UV-defined flat PDMS stamps suitable for microcontact printing. *Langmuir* **2009**, *26*, 3739−3743.
(63) Schnyder, B.; Lippert, T.; Kötz, R.; Wokaun, A.; Graubner, V.-M.; Nuyken, O. UV-irradiation induced modification of PDMS films investigated by XPS and spectroscopic ellipsometry. *Surf. Sci.* **2003**, *532*−*535*, 1067−1071.
(64) Zhou, J.; Voelcker, N. H.; Ellis, A. V. Simple surface modification of poly(dimethylsiloxane) for DNA hybridization. *Biomicrofluidics* **2010**, *4*, 046504.
(65) Sartenaer, Y.; Dreesen, L.; Humbert, C.; Volcke, C.; Tourillon, G.; Louette, P.; Thiry, P. A.; Peremans, A. Adsorption properties of decyl thiocyanate and decanethiol on platinum substrates studied by sum-frequency generation spectroscopy. *Surf. Sci.* **2007**, *601*, 1259−1264.
(66) Gabler, C.; Tomastik, C.; Brenner, J.; Pisarova, L.; Doerr, N.; Allmaier, G. Corrosion properties of ammonium based ionic liquids evaluated by SEM-EDX, XPS and ICP-OES. *Green Chem.* **2011**, *13*, 2869−2877.
(67) Haihua, T. Organic Functionalization of Silicon Surfaces with Alcohols, Ketones and Isothiocyanates. Ph.D. Dissertation, National University of Singapore, Singapore, 2008.